

CP 114

C.P. No. 174  
(13,424)

A.R.C. Technical Report

NATIONAL AERONAUTICAL RESEARCH COUNCIL  
LIBRARY

27 OCT 1954



**MINISTRY OF SUPPLY**

AERONAUTICAL RESEARCH COUNCIL

CURRENT PAPERS

**A Note on the Boundary Layer and Stalling  
Characteristics of Aerofoils**

By

D. D. Carrow, D.F.C., B.A.  
Cambridge University Aeronautics Laboratory

LONDON. HER MAJESTY'S STATIONERY OFFICE

1954

TWO SHILLINGS NET



A Note on the Boundary Layer and Stalling  
 Characteristics of Aerofoils  
 - By -  
 D. D. Carrow, D.F.C., B.A.  
 Cambridge University Aeronautics Laboratory

---

5th October. 1950

SUMMARY

A qualitative explanation is suggested for the changes which occur in the stalling characteristics of aerofoils as the Reynolds number is increased. This explanation is based on the variation, with Reynolds number, in the state of the boundary layer along the upper surface at just below the stalling incidence.

---

1. Introduction

Recent investigations (References 1, 2, 3) into the nature of the boundary layer along the upper surface of an aerofoil at just below the stalling incidence have indicated that the initial breakdown of flow at the stall may, in certain cases, originate from the boundary layer transition region.

A study has therefore been made of the effects of Reynolds number and of aerofoil incidence (i.e., pressure distribution) on the type and position of this transition region.

Explanations, involving a knowledge of the boundary layer conditions, are suggested for the mechanism of the breakdown of flow in five major types of stall, stalling characteristics being classified into these five types according to the manner in which the flow separation at the stall develops.

The variation, for a given aerofoil, of  $C_L$  max with the type of stall is discussed.

Finally, using the results of the above arguments, examples are given of the effect of Reynolds number and of leading edge roughness on the stalling characteristics of several aerofoils, the change from one type of stall to another being explained, in each case, by an alteration in the type of transition region.

The present note is based on an unpublished internal Cambridge University Aeronautics Laboratory Report, which has been revised as a result of advice and encouragement from Dr. J. H. Preston.

## 2. Notation

$U_0$	=	free stream velocity
$U$	=	local velocity over aerofoil at edge of boundary layer
$\nu$	=	kinematic viscosity
$x$	=	distance around upper surface of aerofoil from front stagnation point
$o$	=	aerofoil chord
$\delta^x$	=	boundary layer displacement thickness
$R_o$	=	$\frac{U_0 o}{\nu}$
$R_x$	=	$\frac{U_0 x}{\nu}$
$R_{\delta^x}$	=	$\frac{U \delta^x}{\nu}$

## 3. Transition

A Transition Region is defined as that region in which the boundary layer velocity profiles lie between those for laminar flow and those for a well developed turbulent flow. It is suggested that transition regions can be divided into two entirely different types, Instability Transition and Bubble Transition. These have entirely different characteristics and will be discussed individually below.

**3.1 Instability Transition.**- Lin's Stability Theory', a development of the earlier Tollmein - Schlichting Theory, and verified experimentally by Schubauer & Skramstadt<sup>5</sup> shows that at any chordwise station, small disturbances in a laminar boundary layer will be amplified or damped depending on:-

- (i) The frequency of the disturbance
- (ii) The shape of the boundary layer velocity profile
- (iii) The boundary layer Reynolds number,  $R_{\delta^x}$ .

Assuming that small disturbances of all frequencies are present, due for example to surface irregularities, noise, vibration, or free stream turbulence, there is, for any given velocity profile, a maximum value of the boundary layer Reynolds number ( $R_{\delta^x \text{ crit}}$ ) for stability; above this value disturbances of certain frequencies will be amplified. The chordwise position at which amplification commences can therefore be fairly accurately predicted, (for details see Ref. 6) although the final breakdown to turbulent flow will take place further downstream, depending on the magnitude of the initial disturbance and the subsequent rate of amplification.

Examples are given, in Ref. 7, of the velocity profiles in this type of transition region.

### 3.2 Bubble Transition

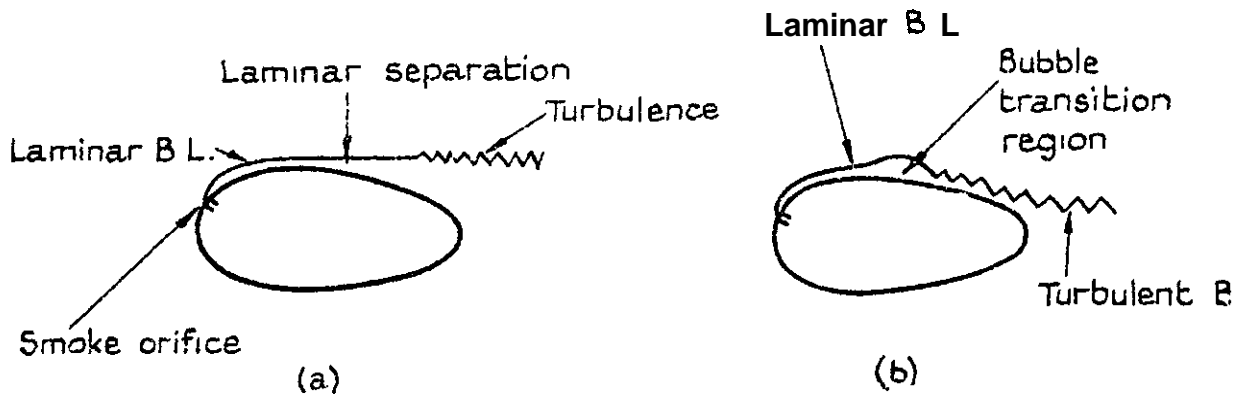


Figure 1

Assuming that no instability transition occurs first (see para. 3.3) laminar separation will take place shortly behind the minimum pressure point on an aerofoil. The rising pressure gradient causes a reversal of flow at the solid surface, undercutting the complete laminar layer, which detaches itself from the surface, still in the laminar condition, but subsequently breaks up, after a short distance, into turbulence. This is shown in Fig. 1(a), which has been taken from an unpublished Cambridge report dealing with flow visualization by means of paraffin smoke issuing from an orifice into the boundary layer.

Fig. 1(b), at a higher Reynolds number than Fig. 1(a), shows how, under certain conditions, the boundary layer reattaches itself a short distance behind the laminar separation point, leaving an intensely turbulent "bubble" under the detached layer; on reattachment the boundary layer is transitional, rapidly becoming fully turbulent. (See also Ref. 8).

Little is known about the conditions required for this reattachment. The results shown in Fig. 1, together with other results on two rather more slender sections, indicate that the bubble first forms at a minimum  $R_x$  of  $5 \times 10^4$ , and that, at this  $R_x$ , the breakdown to turbulence in the detached laminar layer has approached very close to the laminar separation point. If the position of this "transition" in the detached layer is the deciding factor for reattachment, then Lin's Stability Theory might be used on the detached laminar layer to calculate  $R_{x_{min}}$ , but other influences, notably the surface curvature and the steepness of the local adverse pressure gradient, also seem to play an important part.

In general, it appears that, providing  $R_x$  is greater than about  $5 \times 10^4$ , and that there is no exceptionally steep adverse pressure gradient or severe curvature, laminar separation will always be followed, after a region of separated flow, by a reattachment in the turbulent condition, i.e., by a bubble transition region.

When the bubble transition region is far aft, separation often extends over a considerable chordwise distance, of the order of  $x/c = 0.1$ . When, however, the bubble is situated in a steep adverse pressure gradient, it shrinks considerably in size and may extend over a chordwise distance of only about  $x/c = 0.002$ , when it will usually escape observation, except with experiments on very large models such as those of References 1, 2 and 3.

Observations of bubble transition, that is, of local separation of flow in the transition region, are given in References 9, 10, 11 and 12. Examples of velocity profiles in a bubble transition region near the nose of an aerofoil at high incidence are given by Gault<sup>2</sup>.

**3.3 Comparison Between the Two Types of Transition.** - The type of transition region found on the upper surface of an aerofoil depends entirely on which of the two sets of necessary conditions, as described above, is satisfied first.

The Bubble Transition region will always start at the laminar separation point, and its position is therefore independent of the Reynolds number  $R_c$ , but moves forward with increasing incidence, until at  $C_L \max$  it lies just behind the suction pressure peak at the nose.

Instability Transition, however, moves forward with increasing  $R_c$  (since for any given chordwise station  $R_{\delta x}$  will increase with  $R_c$ ). In addition, instability transition will depend on the stability ( $R_{\delta x \text{ crit}}$ ) of the boundary layer velocity profiles.

Now the velocity profiles in an adverse pressure gradient just ahead of laminar separation are most unstable, i.e., they have a very low value of  $R_{\delta x \text{ crit}}$ . Hence the instability transition condition,  $R_{\delta x} > R_{\delta x \text{ crit}}$ , will usually be satisfied ahead of the laminar separation point, so that bubble transition can only be expected when the value of  $R_x$  at the laminar separation point is very low ( $R_{\delta x} < R_{\delta x \text{ crit}}$ ).\* &This means that, if the laminar separation

point/

---

\*N.B. To simplify the argument here, it has been assumed that instability transition commences at the point where  $R_{\delta x} = R_{\delta x \text{ crit}}$ . As discussed in para. 3.1, this is not quite true in practice, instability transition actually commencing rather downstream of this point.

point is far aft, then bubble transition will only occur at fairly low values of  $R_c$ ; alternatively, at high values of  $R_c$  bubble transition will only occur when the laminar separation point is well forward in the very thin boundary layer just behind the front stagnation point.

#### 4. Types of Stall

Stalling characteristics can be classified into five major types depending on the manner in which the stall develops. These are discussed separately below, and explanations are suggested for the mechanism of the breakdown of flow in each case.

##### 4.1 Type. Laminar Separation Moving Forward from the Rear

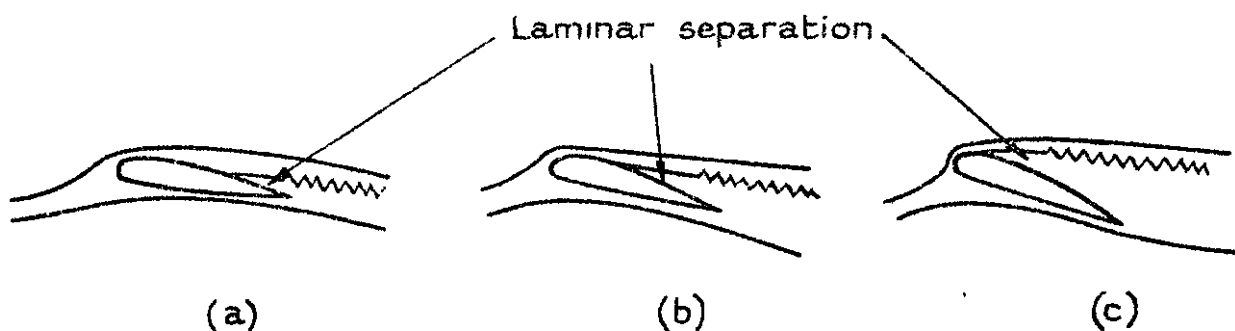


Figure 2.

At low Reynolds numbers, complete separation of the laminar boundary layer from the upper surface takes place just behind the minimum pressure region. The detached layer subsequently breaks down into turbulence, but does not rejoin the surface as a turbulent boundary layer. At zero incidence this separation is well aft, but as the incidence increases, it moves forward, giving a very gentle stall, with a well rounded peak to the Lift Curve.

An example of this type of stall is given by Farren in Ref. 13 and sketches of a typical Type I stall development are given in Fig. 2.

4.2 Type II. Laminar Separation at the Leading Edge

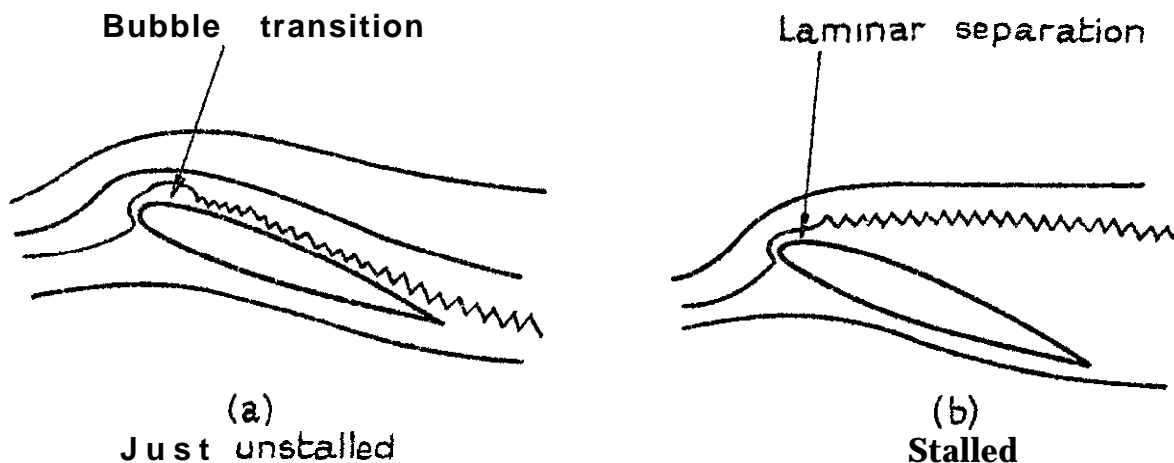


Figure 3

At a higher value of  $R_c$  than for Type I, a Bubble Transition region commences at the laminar separation point and, after reattachment, the turbulent boundary layer continues along the aerofoil surface, With increasing incidence the bubble moves forward until it is situated just behind the leading edge. The stall is now most abrupt and is due to a sudden failure of the boundary layer to reattach itself (possibly due to an excessive suction pressure peak), and the flow separates from the entire upper surface with a sudden and discontinuous drop from CL max in the Lift Curve.

This type of separation is different from Type I (and also as will be seen, from Types III and IV). In a Type I stall, the separation is "reversible" in that small changes in incidence cause the separation point to move to and fro along the surface, giving small changes in the flow pattern. In a Type II stall, however, an "irreversible" change occurs in the whole flow pattern, and once the stall has taken place, the incidence must often be reduced several degrees before the aerofoil unstalls. This "hysteresis" is common with Type II stalls, but is sometimes masked by excessive tunnel turbulence, leading to an unstable, rather than to a hysteretical, range of incidence.

A thorough investigation of this type of stall has been made by Gault and McCullough<sup>1,2</sup>, where, at  $R_c = 5.8 \times 10^6$ , the bubble was only evident after the formation of the leading edge suction pressure peak, i.e., when transition had moved close to the leading edge. At lower incidences the laminar separation point was far back and, as discussed in Section 3.3, instability transition occurred first.

4.3 Type III. Rearward Expansion of the Bubble Transition Region

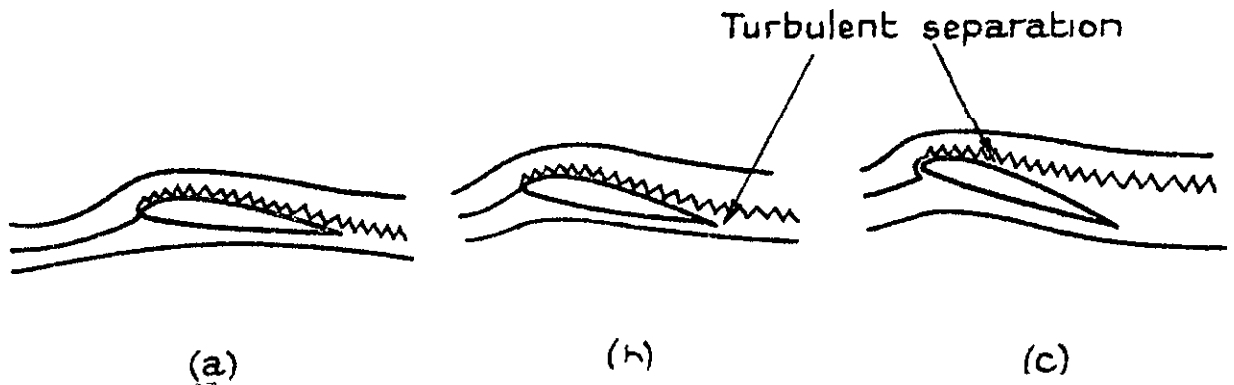


Figure 4.5

For aerofoils having a very severe change of curvature at or near the leading edge, a high suction pressure peak forms over the nose at a relatively low incidence (about  $5^\circ$ ). A Bubble Transition region moves forward to the leading edge, where it appears to 'fair off', the change of curvature, having sufficient effect on the potential flow to reduce greatly this suction peak. There is therefore a noticeable reduction in lift slope just at the incidence where the bubble first forms over the nose. With further increase of incidence, a complete and abrupt laminar separation, as in Type II, does not take place (possibly because the adverse pressure gradient is not now sufficiently steep) and the bubble expands gradually towards the trailing edge, eventually extending over the entire upper surface. The stall is therefore gentle, with a rounded CL peak, and there is a kink in the Lift Curve at the angle of attack where the bubble first reaches the leading edge, although at high Reynolds numbers this kink is not very noticeable and may get faired out in the plotting.

The first complete observations of the nature of the flow with this type of stall have been given by McCullough and Gault<sup>3</sup>. Sketches of the development of the stall are given in Figure 4.

4.4 Type IV. Turbulent Separation Moving Forward from the Rear

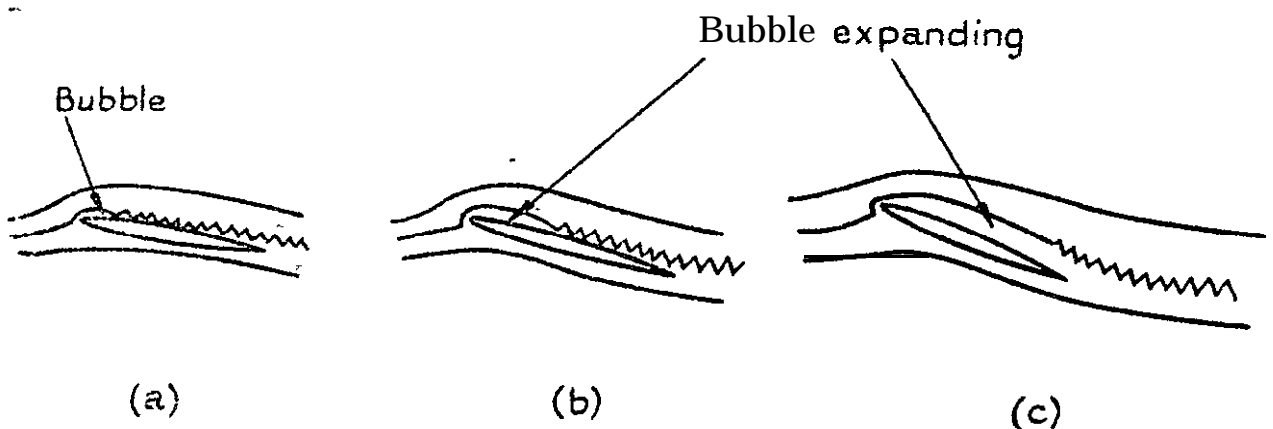


Figure 4.4

With/

With all aerofoils, at a high enough Reynolds number, instability transition will occur ahead of any bubble transition, so that, at high incidences, a turbulent boundary layer will be formed right from the leading edge, and the stall will be then due to turbulent separation moving forward from the trailing edge, with a fairly gentle stall. The development of this type of stall is shown in Figure 5.

It should be noted, however, that conditions sometimes arise where turbulent separation from the trailing edge causes the stall, even though there may be a Bubble Transition near the nose as in Type II, or a Bubble Transition expanding rearwards from the nose as in Type III. This only happens however with very thick and/or highly cambered sections, where, as described in Ref. 14, there is "a race between the development of conditions which cause complete separation from the front of the profile and of those which cause separation towards the rear".

#### 4.5 Turbulent Separation from Near the Leading Edge on Roughened Aerofoils

There is some evidence to suggest that, when the leading edge is roughened, a sudden turbulent separation may in some cases take place near the nose, with a consequent discontinuity in the Lift Curve at the stall which is very similar in appearance to a Type II Stall.

This type of stall is most marked on very thick aerofoils, for example the NACA 65,421 section in Ref. 15 where the gentle Type IV stalls of the smooth aerofoils are changed by roughness into a very abrupt type (see Fig. 6).

One would expect thick aerofoils to be most susceptible to this type of stall, since the suction pressure peak is relatively far aft, and therefore the adverse pressure gradient aft of this peak acts on a relatively thick and fully developed turbulent layer.

This Type V stall has, however, no direct experimental evidence for its existence, and will therefore not be discussed further.

### 5. Comparative Effects of the Type of Stall on $C_L$ max. Other Factors -Remaining a 1

5.1 With a Type I stall,  $C_L$  max is comparatively low, owing to the very early laminar separation which spreads from the rear as the incidence increases.

5.2 With a Type III stall,  $C_L$  max is higher than Type I, but still rather low, owing to the early separation spreading aft from the nose and enclosing a region of almost constant and comparatively high pressure.

5.3 With a Type II stall, a given aerofoil will reach a much higher  $C_L$  max than with Types I or III, because a very high suction peak forms over the leading edge before the stall, so that considerably more lift is obtained.

5.4 With a Type IV stall, the highest possible  $C_L$  max will be reached, since the stalling conditions will be governed by turbulent separation spreading forward from the trailing edge; this means that a higher incidence will be reached than in the case of the Type II stall, where trailing edge turbulent separation has not yet started (or only just started) when separation from the leading edge takes place.

5.5 A Type V stall will not give quite as high a  $CL_{max}$  as Types II or IV owing to the greatly increased boundary layer thickness due to the leading edge roughness; the stalling incidence is also usually slightly lower.

## 6. Examples of the Change in Stalling Characteristics with Reynolds Number and with Leading Edge Roughness

The type of stall which takes place at any given Reynolds number  $R_c$  can usually be determined by an examination of the appropriate Lift Curve, and, if Lift Curves are available over a range of  $R_c$ , a critical  $R_c$  is often found, in the region of which the stalling characteristics change from one type to another. Some examples are given below.

Examples I to V are for a number of straightforward cases, where there is a marked change in the type of stall, following an alteration in the condition of the boundary layer due either to increasing  $R_c$  or to the addition of leading edge roughness.

Examples VI and VII are typical of the rather mixed conditions occurring at the stall of thick and highly cambered aerofoils, for the reasons mentioned previously in section 4.4.

### 6.1 Example I. Change from Type I to Type II and from Type II to Type IV with Increasing $R_c$

This example is typical of medium thickness low camber sections.

In Fig. 7(a) taken from Ref. 16 MCA 0009 has a very rounded  $C_L$  peak up to  $R_c = 6.65 \times 10^5$ , where it appears to be on the point of changing to the abruptly discontinuous type found at higher  $R_c$ . Fig. 7(b) from the same reference, shows the changeover at  $R_c \sim 5 \times 10^5$  for the NACA 0042 section. Again, in Fig. 8, taken from Ref. 17 for the NACA 63-009 and 64-009 sections, it is seen that this abruptness at the stall persists up to  $R_c = 15 \times 10^6$ , but has disappeared at  $R_c = 15 \times 10^6$  and above. Thus one deduces for the NACA 0009 section approximately:-

- (a) Type I stall  $R_c < 6 \times 10^5$ .
- (b) Type II stall  $6 \times 10^5 < R_c < 12 \times 10^5$ .
- (c) Type IV stall  $R_c > 12 \times 10^5$ .

Reference 2 confirms the existence of a Type II stall on the NACA 63-009 aerofoil at  $R_c = 5.8 \times 10^6$ .

### 6.2 Example II. Change from Type II to Type IV with increasing $R_c$

This example is typical of very thick sections. In Reference 18, a change from a Type II to a Type IV stall occurs, for several very thick sections, at around  $R_c = 3 \times 10^5$ . This critical Reynolds number is much lower than for the thinner section of example I, which is to be expected, since on these thick sections the peak suction is further aft and so instability transition moves upstream of the laminar separation point at a much lower value of  $R_c$ . Fig. 9 is taken from Ref. 18.

Further confirmation of the above deductions comes from the behaviour of  $CL_{max}$ , which, in the region above  $R_c$  crit, decreases steadily with increasing  $R_c$ , showing the effect of the instability

transition/

transition moving forward with increasing  $R_c$  to give a greater extent of turbulent boundary layer, thus decreasing the effective camber and also increasing the tendency towards an earlier trailing edge turbulent separation.

### 6.3 Example III. Change from Type III to Type IV with Increasing $R_c$

- (a) Results on circular back aerofoils<sup>19</sup> indicate by the kink in the Lift Curve at a relatively low incidence that a Type III stall occurs on these sections from the lowest tested  $R_c$  of  $10^5$  up a critical  $R_c$  of about  $4 \times 10^6$ , at which value the stalling characteristics change to Type IV.
- (b) Similar results to the above are observed for the NACA 63-006 section<sup>17</sup> where there is a large increase of CL max at about  $R_c = 9 \times 10^6$  showing a change from Type III to Type IV in this region, and this is confirmed by Ref. 3, which gives for the NACA 64A006 section, a Type III stall at  $R_c = 5.8 \times 10^6$ . This example is typical of all very thin aerofoils.

### 6.4 Example IV. Change from Type II to Type IV due to Leading Edge Roughness.

Many examples are given in Ref. 15 at  $R_c = 6 \times 10^6$  of the effect of leading edge roughness on medium thickness (9%-15%) aerofoils. A Type IV std.1 is obtained, due to instability transition being right forward, but CL max is lowered because of the greatly thickened boundary layer. An example is shown in Fig. 10 for the NACA 63-210 aerofoil at  $R_c = 6 \times 10^6$ .

### 6.5 Example V. Change from Type III to Type IV due to Leading Edge Roughness

On all thin (6%) aerofoils given in Ref. 15, the effect of leading edge roughness is actually to increase CL max, in contrast to Example IV. The Lift Curve peak remains rounded and the change is from a Type III to a Type IV stall. An example, the NACA 65-006 aerofoil, is shown in Fig. 11.

### 6.6 Example VI. Mixed Stalling Characteristics

Pinkerton<sup>20</sup> gives details of the pressure distribution over a NACA 4412 section. Replacing the "effective" Reynolds number as used in this reference by the actual Test Reynolds number, it will be seen that up to  $R_c = 3.41 \times 10^5$ , separation is chiefly due to a Type II stall, the bubble transition region being most clearly defined by the uniform pressure region near the nose. There is, however, some separation, or at any rate undue thickening of the turbulent boundary layer, at the trailing edge as well, so that the final stall, although it shows the typical Type II collapse of the leading edge pressure peak, does not give such a severe drop in  $C_L$  as if there had been no turbulent separation at the trailing edge. At  $R_c = 6.8 \times 10^5$  (Test  $R_c$ ) and above, however it will be seen that evidence of a bubble transition near the leading edge has disappeared and the stall is a straightforward Type IV, with a gradual collapse of the leading edge pressure peak as turbulent separation moves forward from the trailing edge.

In/

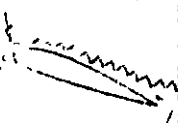
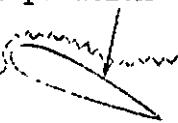
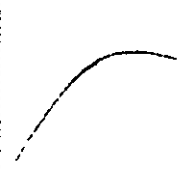
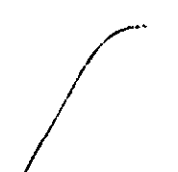
In this same report, Pinkerton suggests that the local laminar separation near the nose is prevented, at high Reynolds numbers, by a transition from laminar to turbulent flow before the laminar flow has reached separation conditions.

#### 6.7 Example VII. Mixed Stalling Characteristics

Observations of the RAF 28 aerofoil section at  $R_c = 1.1 \times 10^5$ , given in Ref. 14, indicate that this aerofoil stalls as a result both of the rearward spread of separation from the bubble transition region at the leading edge (as in a Type III stall) and also of the forward spread of turbulent separation from the trailing edge (as in a Type IV stall).

#### 7. Summary of Stalling Characteristics/

7. Summary of Stalling Characteristics

Type	I	II	III	IV	V
Description	Laminar separation moving forward from the rear	Laminar separation at the leading edge	Rearward expansion of the bubble transition region	Turbulent separation moving forward from the rear	Turbulent separation from near the L.E. on roughened aerofoils
Diagram of boundary layer just before stall	 moving forward	 turbulent layer	 of bubble	 turbulent separation	
Typical Lift Curve Incidence					
Remarks	Unimportant Only occurs at very low $R_c$ .	Undesirable Discontinuous stall	Severe change of curvature at nose	All aerofoils to this type at high enough $R_c$	For very thick end roughened aerofoils. Rather hypothetical.
Examples	NACA 0009 $R_c < 6 \times 10^5$ (Section 6.1)	NACA 0009 $6 \times 10^5 < R_c < 12 \times 10^5$ (Section 6.1)	NACA 63-006 $R_c < 9 \times 10^5$ (Section 6.3)	NACA 0009 $R_c > 12 \times 10^5$ (Section 6.1)	NACA 65 <sub>L</sub> 421 $R_c = 6 \times 10^5$ smooth. (Section 4.5)
					NACA 65 <sub>L</sub> 421 $R_c = 6 \times 10^5$ rough. (Section 4.5)

## 8. Discussion and Conclusions

8.1 It is hoped that sufficient **examples** have been given to show that the ideas presented in this **note** are of reasonably **wide** significance. Although there **are** many aerofoils whose stalling characteristics do not fit exactly into one of the five types discussed above, it **is** thought that these characteristics will, if investigated, **always** prove to be a mixture of **two** types, **as** in examples VI **and** VII.

8.2 Many of the thin, **low** cambered sections, now coming into **wide** use for **high** speed aircraft, have stalling **characteristics** that can be **exactly** **classified** in terms of Types II, III **and** IV.

For **medium** thickness sections the critical Reynolds number for the **change** from Type II to Type IV is around  $R_c = 15 \times 10^6$ , so that the **undesirable** Type II stall will be present at the landing speeds of such aircraft. In **the** past, however, surface irregularities on the **acrofoil** caused early instability transition which prevented the development of the Type II stall, giving **instead** the satisfactory Type IV. Trouble from the Type II stall at Flight Reynolds **numbers** has therefore only **recently** become evident, owing to the development of **very** smooth "laminar flow" aerofoil surfaces.

8.3 Excessive leading edge roughness will reduce  $CL_{max}$  due to the greatly thickened turbulent **boundary layer**, and may **even**, on the thickest sections, promote the undesirable Type V **stall**. However **it** appears that the **careful** use of a very small spoiler - almost a roughness element - placed **spanwise** **very** close to the front stagnation point, might well induce a Type IV stall, **with** rounded Lift peak, in preference to a Type II stall, **without** greatly thickening the boundary layer and so reducing  $CL_{max}$ . There might even, as discussed in Section 5.4, be a slight gain in  $CL_{max}$ . For very **thin** aerofoils the lift peak **would** **remain** rounded and there would be a distinct increase of  $CL_{max}$  due to the stall **changing** from Type III to Type IV.

In order to give the maximum area of laminar flow at high speed, this spoiler might have to be retractable. **However**, since at low **incidences** it would be situated in a very **favourable** pressure gradient, a critical size of spoiler might be so **arranged** **as** not to disturb the flow under these **favourable** conditions, so that no retraction would be necessary.

8.4 Most of the ideas and **explanations** presented are rather speculative and **more** experimental **results** are required, particularly **acrofoil** data **obtained** in low turbulence tunnels, since excessive free **stream** turbulence, like **surface** roughness, will cause an early instability transition **resulting** in a Type IV stall at a **much** lower  $R_c$  in the tunnel than in free flight. **Experiments** are also required on the factors effecting the formation of bubble **transition** and its breakdown under **adverse** conditions. This would probably best be accomplished by flow visualization studies, using a smoke filament or china **clay** technique<sup>21</sup>. The **importance** of flow visualization in obtaining an **understanding** of the **stall** cannot be over-emphasized.

The eventual **aim** of all the experiments would be to eliminate the Type II stall completely by **careful** aerofoil design and to ensure that a Type IV stall took place under **all** Flight **Conditions**.

9. References

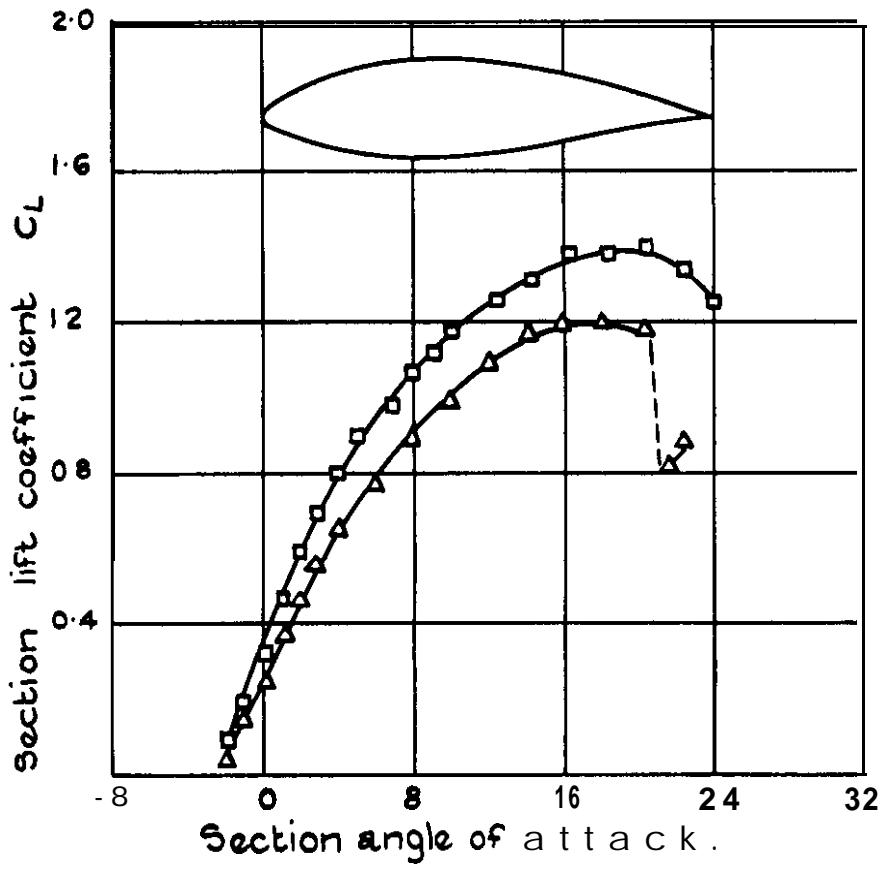
<u>No.</u>	<u>Author(s)</u>	<u>Title. etc.</u>
1	McCullough, George B. Gault, Donald E.	An <b>experimental</b> investigation of an NACA 63 <sub>1</sub> -012 airfoil <b>section with leading edge suction</b> slots, N.A.C.A. Tech. Note.1683, 1948.
2	Gault, Donald E.	Boundary layer end <b>stalling</b> characteristics of the NACA 63-009 airfoil section. N.A.C.A. Tech. Note 1894, 1949.
3	McCullough, George B. Gault, Donald E.	Boundary <b>layer and</b> stalling characteristics of the NACA 64A006 airfoil section. N.A.C.A. Tech. Note 1923, 1949.
4.	Lin, c. c.	On the stability of <b>two-dimensional</b> parallel flows. Qu. App. Maths. Vol.III, pp.117-142, pp.218-234, pp.277-301. 1945-1946.
5	Schubauer, G. B. Skramstad, n. K.	<b>Laminar</b> boundary <b>layer</b> oscillations end transition on a flat plate. N.A.C.A. Tech. Rep.909, 1948.
6	Hahneman, E. Freeman, J. C. Finston, M.	Stability of boundary layers end of flow in entrance <b>section</b> of a <b>channel</b> . Jour. Acro. Sci. 1948, pp.493-496.
7	Silverstem, Abe. Becker, John V.	Determination of boundary layer transition on three <b>symmetrical</b> airfoils in the NACA full scale <b>wind</b> tunnel. N.A.C.A. Tech Rep. 637, 1939.
8	Liepmann, Hans W. Fila, Gertrude II.	Investigations of effects of surface temperature and <b>single</b> roughness elements on boundary <b>layer</b> transition. N.A.C.A. Tech, Rep, 890, 1947.
9	Schubauer, G. B.	Air flow in the boundary <b>layer</b> of an <b>elliptic cylinder</b> . N.A.C.A. Tech. Rep, 652, 1939.
10	Page, A. Preston, J. H.	On transition from <b>laminar</b> to turbulent flow in the boundary layer. Proc. Roy. Soc.A. No.973, Vol.178, pp.201-227, June 1941.
11	Batson, A. S. Preston, J. H.	The effect of boundary layer <b>thickness on</b> the normal force distribution of <b>aerofoils</b> , with particular reference to control problems. R. & M., 2008, 1942.

References (Continued)

<u>No.</u>	<u>Author(s)</u>	<u>Title etc.</u>
12	Preston, J. H. Sweeting, N. E. Cox, Miss D. K.	The experimental determination of the two-dimensional interference on a large chord Piercy 12/40 aerofoil in a closed tunnel fitted with a flexible roof end floor. R. & M. 2007, 1944.
13	Fen-en, W. S.	Air flow. With demonstrations on the screen by means of smoke. Jour. Roy. Aero. Soc. No. 36, 1932, p. 466, Fig. 14.
14	Aeronautics Laboratory, Cambridge	An experimental study of the stalling of wings. R. & M. 1588, 1934.
15	Abbott and Von Doenhoff	Theory of wing sections. McGraw Hill, 1949.
16	Jacobs, Eastman N. Sherman, Albert	Airfoil section characteristics as affected by variations in the Reynolds number. N.A.C.A. Tech. Rcp. 586, 1937.
17	Loftin, Laurence K. Bursnall, William J.	The effects of variations in Reynolds number between $3.0 \times 10^5$ and $25.0 \times 10^6$ upon the aerodynamic characteristics of a number of NACA 6-Series airfoil sections. N.A.C.A. Tech. Note 1773, 1948.
18	Jacobs, Eastman N.	The aerodynamic characteristics of eight very thick aerofoils from tests in the variable density wind tunnel. N.A.C.A. Tech. Rep. 391, 1931.
19	Williams, D. H. Brown, A. F. Inles, C. J. W.	Tests on four circular-back aerofoils in the Compressed Air Tunnel. R. & M. 2301, 1948.
20	Pinkerton, Robert M.	The variation with Reynolds number of pressure distribution over an aerofoil section. N.A.C.A. Tech. Rep. 613, 1938.
21	Preston, J. H.	Visualization of boundary layer flow. R. & M. 2267, 1946.

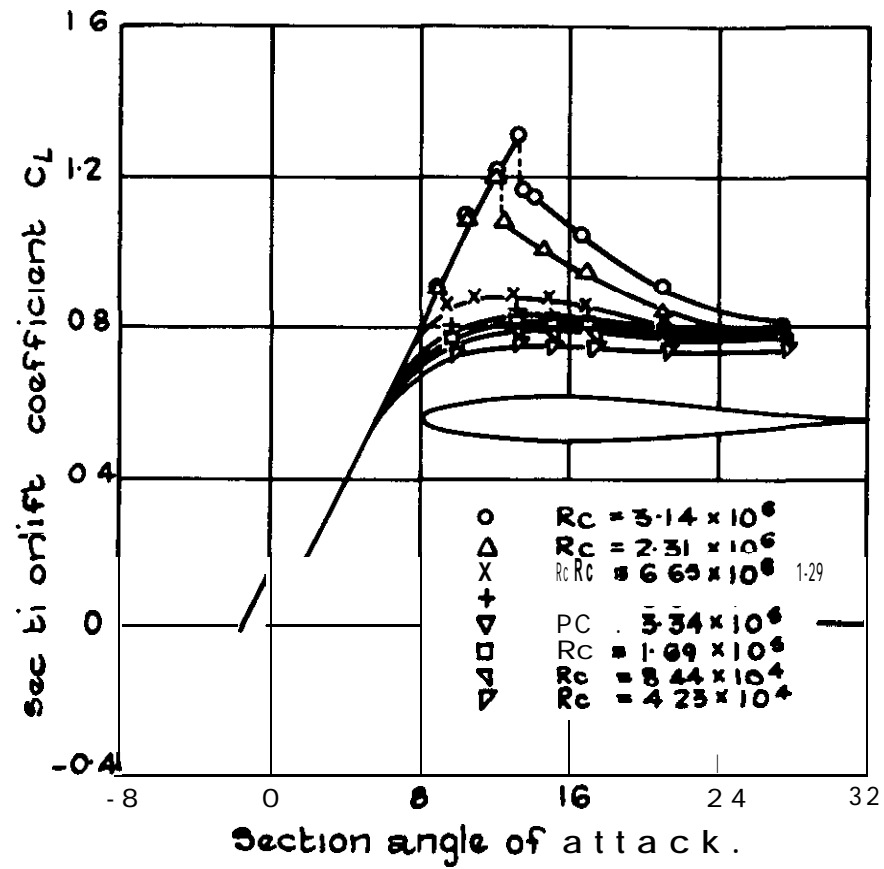
---



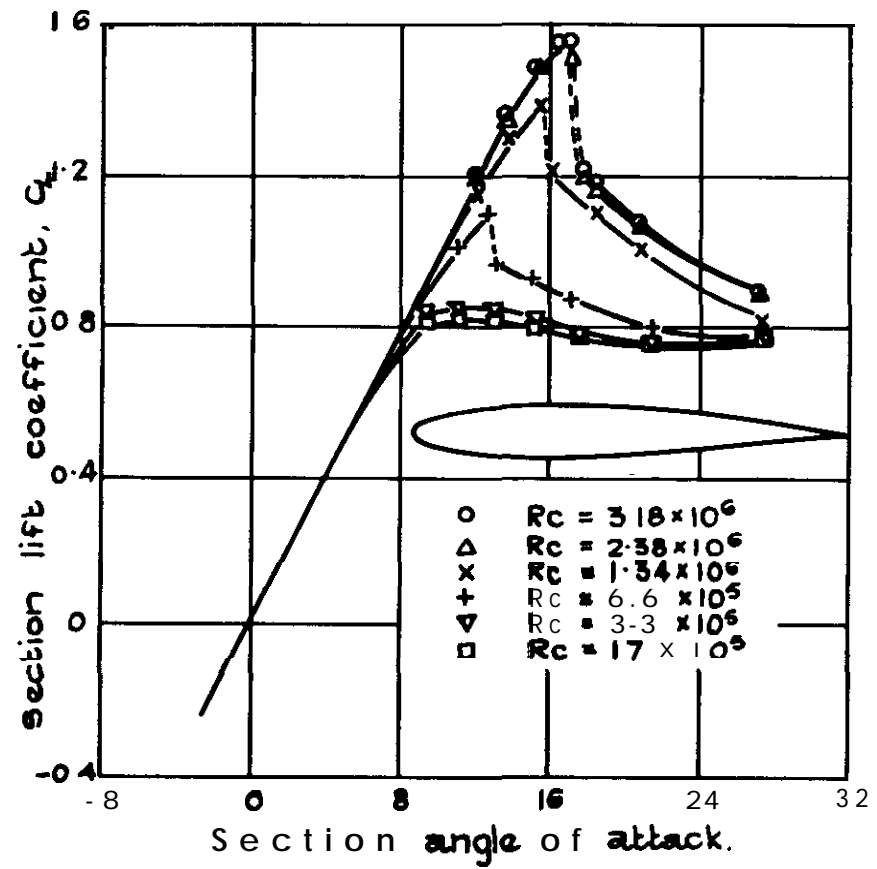


□  $R_c = 6.0 \times 10^6$  Smooth  
 ▲  $R_c = 60 \times 10^6$  Standard roughness

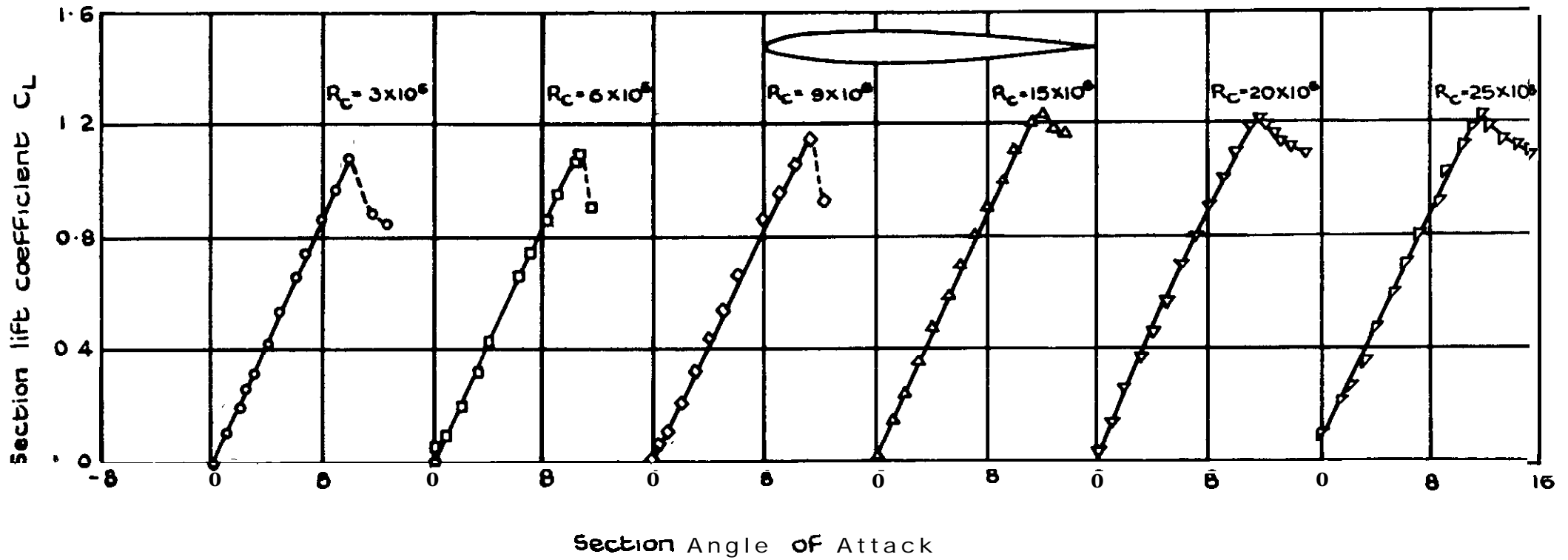
N.A.C.A 6 5 4 421 Wing Section.



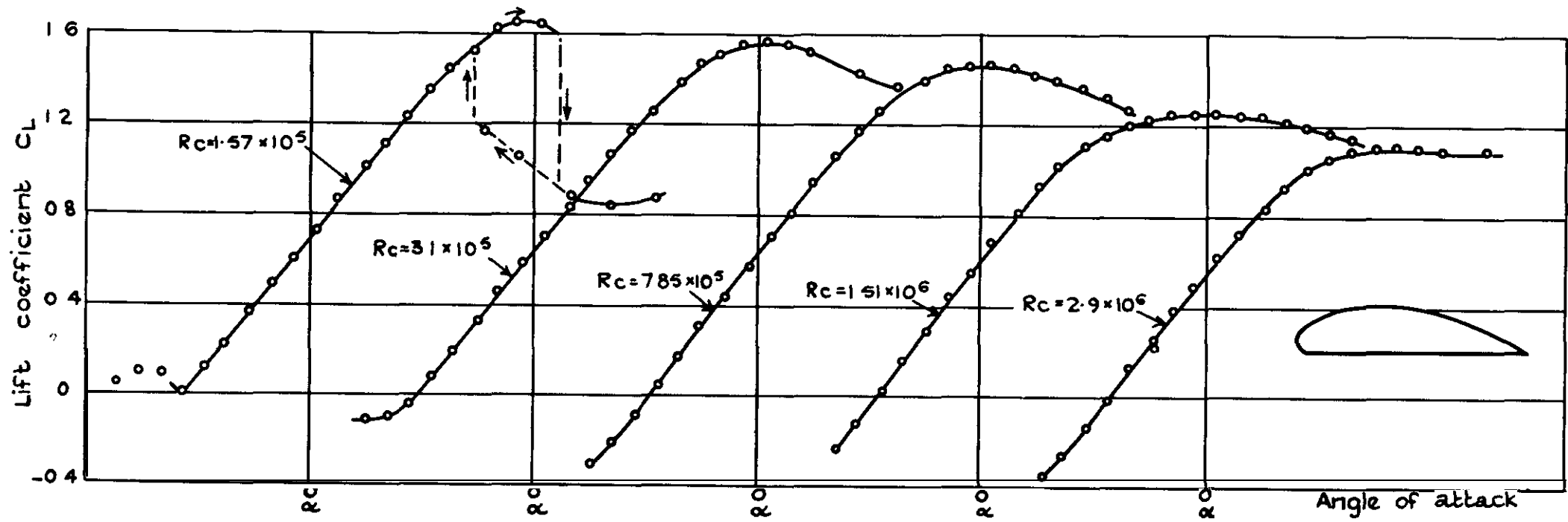
(a) N.A.C.A. 0009 Wing Section



(b) N.A.C.A. 0012 Wing Section



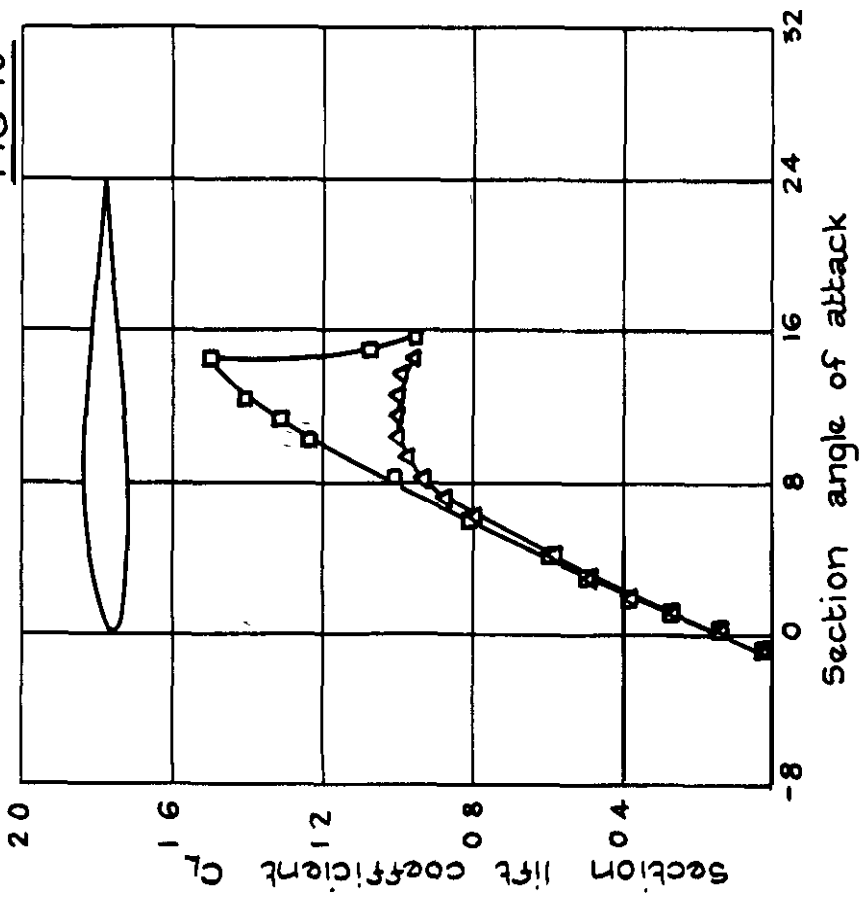
NACA 63 - 00 9 Aerofoil (NACA 64 - 0 0s very similar)



Variation of  $C_L$  with Reynolds No

NACA 103 Aerofoil

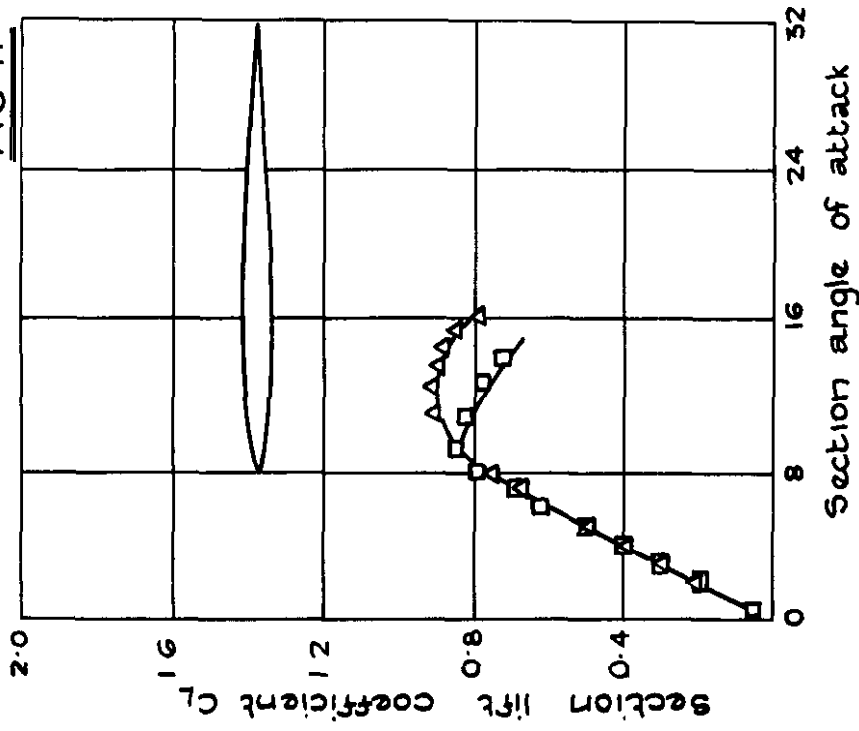
FIG 10



□  $R_c = 6.0 \times 10^6$  smooth  
 △  $R_c = 6.0 \times 10^5$  standard roughness

N.A.C.A. 63-210 Wing Section

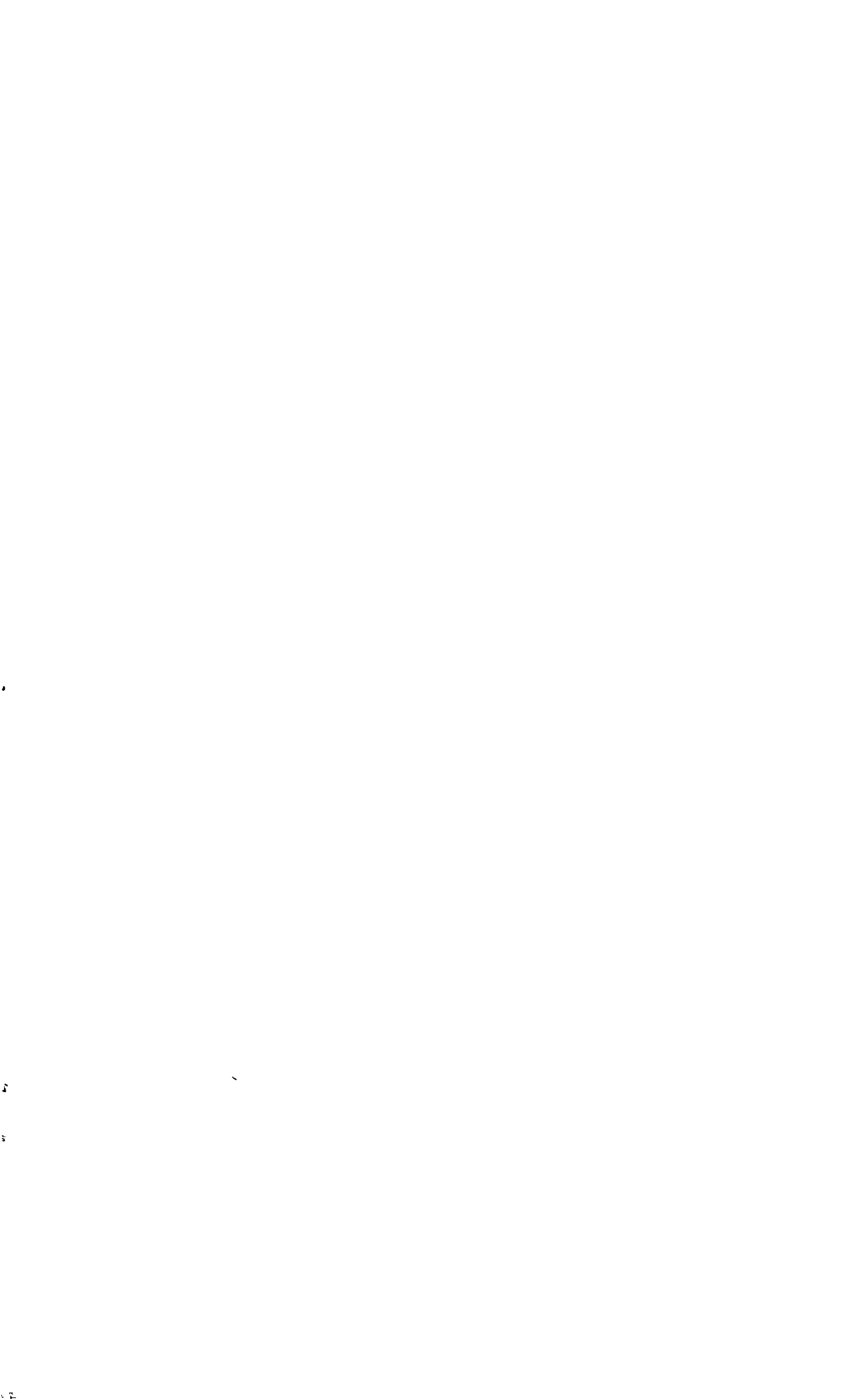
FIG 11



□ smooth  
 △ standard roughness

N.A.C.A. 65-006 Wing Section





*CROWN COPYRIGHT RESERVED*

**PRINTED AND PUBLISHED BY HER MAJESTY'S STATIONERY OFFICE**

**To be purchased from**

York House, **Kingsway, LONDON, W C 2**    423 Oxford Street, **LONDON, W 1**  
PO Box 569. **LONDON, se.1**

**13a Castle Street, EDINBURGH, 2**    **1 St Andrew's Crescent, CARDIFF**  
**39 King Street, MANCHESTER, 2**    Tower Lane. **BRISTOL, 1**  
**2 Edmund Street, BIRMINGHAM, 3**    **50 Chichester Street, BELFAST**

**Or from any Bookseller**

1954

**Price 2s 0d net**

**PRINTED IN GREAT BRITAIN**